

REPORT DOCUMENTATION PAGE

Form Approved
OMB No. 0704-0188

AD-A238 411



estimated to average 1 hour per response, including the time for reviewing instructions, searching existing data sources, gathering the collection of information. Send comments regarding this burden estimate or any other aspect of this report, to Washington Headquarters Services, Directorate for Information Operations and Reports, 1215 Jefferson Avenue, Office of Management and Budget, Paperwork Reduction Project (0704-0188), Washington, DC 20503.

REPORT DATE

3. REPORT TYPE AND DATES COVERED

REPRINT

Self-consistent far-infrared response of quantum-dot structures.

5. FUNDING NUMBERS

DAAL 03-90-G-0015

6. AUTHOR(S)

D. A. Broido, K. Kempa, and P. Bakshi

7. PERFORMING ORGANIZATION NAME(S) AND ADDRESS(ES)

Department Of Physics
Boston College
Chestnut Hill
MA 021678. PERFORMING ORGANIZATION
REPORT NUMBER

9. SPONSORING/MONITORING AGENCY NAME(S) AND ADDRESS(ES)

U. S. Army Research Office
P. O. Box 12211
Research Triangle Park, NC 27709-221110. SPONSORING/MONITORING
AGENCY REPORT NUMBER

ARO 26682.6-PH

11. SUPPLEMENTARY NOTES

The view, opinions and/or findings contained in this report are those of the author(s) and should not be construed as an official Department of the Army position, policy, or decision, unless so designated by other documentation.

12a. DISTRIBUTION/AVAILABILITY STATEMENT

Approved for public release; distribution unlimited.

12b. DISTRIBUTION CODE

13. ABSTRACT (Maximum 200 words)

We develop a first-principles, self-consistent theory of the far-infrared (FIR) electromagnetic response for electrons confined in a quantum dot. We find that for small electron number n_e , the FIR absorption spectrum corresponds to that associated with parabolic confinement, i.e., absorption dominated by a single peak, which occurs at the frequency corresponding to the interlevel separation of the parabolic potential, and is roughly independent of n_e . For large electron number, an upward shift in the resonance frequency occurs as the electron density probes the increasingly nonparabolic curvature of the dot potential. Effects of an applied magnetic field are also investigated.

91-05510



14. SUBJECT TERMS

Far infrared response
Self consistent Electromagnetic Response
Quantum dots

15. NUMBER OF PAGES

16. PRICE CODE

17. SECURITY CLASSIFICATION
OF REPORT

UNCLASSIFIED

18. SECURITY CLASSIFICATION
OF THIS PAGE

UNCLASSIFIED

19. SECURITY CLASSIFICATION
OF ABSTRACT

UNCLASSIFIED

20. LIMITATION OF ABSTRACT

UL

Reprinted from

PHYSICAL REVIEW B

CONDENSED MATTER

Volume 42

Third Series

Number 17

15 DECEMBER 1990

I

Self-consistent far-infrared response of quantum-dot structures

D. A. Broido, K. Kempa, and P. Bakshi

Physics Department, Boston College, Chestnut Hill, Massachusetts 02167-3811

pp. 11400-11403

Published by

THE AMERICAN PHYSICAL SOCIETY

through the

AMERICAN INSTITUTE OF PHYSICS



Self-consistent far-infrared response of quantum-dot structures

D. A. Broido, K. Kempa, and P. Bakshi

Physics Department, Boston College, Chestnut Hill, Massachusetts 02167-3811

(Received 23 July 1990; revised manuscript received 4 September 1990)

We develop a first-principles, self-consistent theory of the far-infrared (FIR) electromagnetic response for electrons confined in a quantum dot. We find that for small electron number n_e , the FIR absorption spectrum corresponds to that associated with parabolic confinement, i.e., absorption dominated by a single peak, which occurs at the frequency corresponding to the interlevel separation of the parabolic potential, and is roughly independent of n_e . For large electron number, an upward shift in the resonance frequency occurs as the electron density probes the increasingly nonparabolic curvature of the dot potential. Effects of an applied magnetic field are also investigated.

With recent advances in nanofabrication technology it has become possible to confine electrons in all three spatial dimensions in semiconductor structures called quantum dots.¹⁻⁴ Such structures are analogous to atoms but, in place of an atomic potential, electrons see the artificially constructed dot potential. Typically, the lateral electron confinement is produced either from periodic etching^{1,3} or periodic gating^{2,4} of a quasi-two-dimensional (2D) electron gas. In the first case, the electrons in each dot are confined by layers of positively charged impurities and, possibly, occupied surface states.¹ In the second case, a gate voltage can effectively be viewed as producing positively charged disks that confine electrons to the dots.

A recent experimental study² of the far-infrared (FIR) electromagnetic properties of quantum dots shows that for zero magnetic field, the FIR absorption spectrum is governed by a single peak whose corresponding frequency is roughly independent of the number of electrons n_e occupying each dot. For nonzero magnetic field, applied perpendicular to the dots, a splitting of the resonance occurs producing two peaks that are also relatively insensitive to changes in n_e . This behavior can be explained⁵⁻⁸ when the potential that confines electrons in a dot is parabolic. However, the parabolicity of the dot potential can be expected to break down when the electron density extends to the edges of the dot. Therefore, a complete theory is needed of the electromagnetic response of a quantum dot that employs a realistic, self-consistently calculated confining potential. In this Rapid Communication we present such a complete approach. Specifically, we calculate self-consistently the FIR electromagnetic response of a GaAs quantum dot, containing between 1 and 30 electrons, without and with an applied magnetic field.

In current dot geometries the dots are well separated so that no overlap between the electronic wave functions in neighboring dots can occur. Furthermore, it has been shown⁸ that the interdot electromagnetic interactions produce a negligible shift in the FIR absorption frequency for most samples studied so far. We therefore assume that each dot is isolated from all others. Also, since the lateral extent of the electron confinement in the dot is typically about ten times larger than that along the growth direction, we model each dot as a two-dimensional system. We also approximate the positive charges⁹ to be uniformly distributed into a jellium. Similar modeling has been used in the case of small metallic clusters,¹⁰ where electrons were taken to be confined by a spherical jellium. We further assume that the dot potential possesses a circular symmetry. This latter assumption has been shown, even for square-shaped dots,¹¹ to be a reasonable approximation. Finally, for mesa-etched dots, electrons that may be trapped in surface states¹ are modeled by a ring of negative charge at the edge of the jellium disk.

The potential energy $V(\mathbf{x})$ of an electron interacting with a charge density $\rho(\mathbf{x})$ in the dot is given by

$$V(\mathbf{x}) = \frac{e}{\kappa} \int \frac{\rho(\mathbf{x}')}{|\mathbf{x} - \mathbf{x}'|} d\mathbf{x}', \quad (1)$$

where $\mathbf{x} = (r, z)$, $\mathbf{r} = (r, \theta)$, and κ is the dielectric constant of the semiconductor. For a jellium disk of radius R and areal density n_+ centered at the origin of the $z=0$ plane the charge density is $\rho_+ = en_+ \delta(z) \theta(R-r)$. For a ring of N_- negative charges in this plane at $r=R$ the corresponding density is $\rho_- = -(eN_-/2\pi r) \delta(r-R) \delta(z)$. The potential energy of an electron interacting with these respective charge densities in the $z=0$ plane is $V(r, 0) = V_+(r) + V_-(r)$, where

$$V_+(r) = -\frac{4e^2}{\kappa} n_+ \times \begin{cases} RE(r/R), & r < R \\ r[E(R/r) - (1 - R^2/r^2)K(R/r)], & r > R; \end{cases} \quad (2a)$$

$$(2b)$$

$$V_-(r) = \frac{2e^2}{\pi} N_- \times \begin{cases} \frac{1}{\kappa R} K(r/R), & r < R \\ \frac{1}{r} K(R/r), & r > R. \end{cases} \quad (3a)$$

$$(3b)$$

In the equations, K and E are the complete elliptic integrals of the first and second kind, respectively.

As a consequence of the circular symmetry, the wave functions for electrons in the $z=0$ plane confined by the dot potential defined by Eqs. (2) and (3), and including a magnetic field, $\mathbf{B}=B\hat{z}$, are separable: $\psi_{n,l}(r) = \psi_{n,l}(r)e^{il\theta}$, with $\psi_{n,l}$ satisfying the Schrödinger equation:

$$\left[-\frac{\hbar^2}{2m_e} \left(\frac{1}{r} \frac{d}{dr} r \frac{d}{dr} \right) + V_{\text{eff}}(r) \right] \psi_{n,l} = \epsilon_{n,l} \psi_{n,l},$$

$$V_{\text{eff}}(r) = V(r) + \frac{\hbar^2 l^2}{2m_e r^2} + \frac{1}{2} m_e \omega_c^2 r^2 + \frac{1}{2} \hbar \omega_c, \quad (4)$$

$$l=0, \pm 1, \pm 2, \dots, \quad \omega_c = \frac{eB}{m_e c}.$$

Here, m_e is the electron effective mass and l is the orbital quantum number. The Zeeman splitting of the electron levels is ignored. The potential, $V(r) = V_+(r) + V_-(r) + V_e(r)$, where $V_e(r)$ is obtained by solving Eq. (1)

$$\chi(r, r') = \sum_{n,l} g_{n,l} \sum_{n',l'+m} \frac{f_{n,l} - f_{n',l'+m}}{\epsilon_{n,l} - \epsilon_{n',l'+m} + \hbar\omega + i\gamma} \psi_{n,l}(r) \psi_{n',l'+m}(r') \psi_{n',l'+m}(r) \psi_{n,l}(r) e^{im(\theta - \theta')}, \quad (7)$$

with $m = l' - l$, $f_{n,l}$ the electron distribution function, and γ a phenomenological broadening factor.

Using the two-dimensional Fourier expansion of $1/|r' - r''|$ and expanding $\delta\rho(r)$ and $\chi(r, r')$ as

$$\delta\rho(r) = \sum_m \delta\rho_m(r) e^{im\theta}, \quad (8)$$

$$\chi(r, r') = \sum_m \chi_m(r, r') e^{im(\theta - \theta')}, \quad (9)$$

$$R_m(r', r'') = \int_0^\infty dq J_m(qr') J_m(qr''),$$

$$= \begin{cases} \frac{(r''/r')^m (r'/2)^{-1} \Gamma((2m+1)/2)}{2\Gamma(m+1)\Gamma(1/2)} {}_2F_1((2m+1)/2, \frac{1}{2}, m+1; (r'')^2/(r')^2), & r'' < r' \\ \frac{(r'/r'')^m (r''/2)^{-1} \Gamma((2m+1)/2)}{2\Gamma(m+1)\Gamma(1/2)} {}_2F_1((2m+1)/2, \frac{1}{2}, m+1; (r')^2/(r'')^2), & r'' > r', \end{cases} \quad (13a)$$

$$= \begin{cases} \frac{(r''/r')^m (r'/2)^{-1} \Gamma((2m+1)/2)}{2\Gamma(m+1)\Gamma(1/2)} {}_2F_1((2m+1)/2, \frac{1}{2}, m+1; (r'')^2/(r')^2), & r'' < r' \\ \frac{(r'/r'')^m (r''/2)^{-1} \Gamma((2m+1)/2)}{2\Gamma(m+1)\Gamma(1/2)} {}_2F_1((2m+1)/2, \frac{1}{2}, m+1; (r')^2/(r'')^2), & r'' > r', \end{cases} \quad (13b)$$

where $J_m(x)$, $\Gamma(x)$, ${}_2F_1(a, b, c; d)$ are, respectively, the Bessel, gamma, and Hypergeometric functions. The hypergeometric function entering Eq. (13) can always be expressed¹³ as a linear combination of the complete elliptic integrals $K(z) = \frac{1}{2} \pi {}_2F_1(\frac{1}{2}, \frac{1}{2}, 1; z^2)$ and $E(z) = \frac{1}{2} \pi {}_2F_1(-\frac{1}{2}, \frac{1}{2}, 1; z^2)$.

It is clear that the solutions of the integral equation, Eq. (10), corresponding to different m are independent. Furthermore, only those modes whose m 's correspond to nonvanishing Fourier components of the external potential [Eq. (11)], couple to the external radiation. For radiation whose wavelength is much larger than the dot size, the external electric field can be considered as spatially uniform. Choosing this field to be polarized along the x

employing the electronic charge density in the dot, $\rho_e(r, z) = -en(r)\delta(z)$, with

$$n(r) = \sum_{n,l} g_{n,l} |\psi_{n,l}|^2, \quad (5)$$

where the sum is over all occupied levels and $g_{nl}=0, 1$, or 2 gives the occupancy of level (n, l) ; we take the temperature, $T=0$ K. The ground state of the system is obtained by self-consistently solving Eqs. (1), (4), and (5).

We now calculate the charge density induced in the system by external electromagnetic radiation of the form $V^{\text{ext}}(r, t) = V^{\text{ext}}(r) \exp(i\omega t)$, where ω is the frequency. We use the general random-phase-approximation (RPA) formula¹² applied to our 2D case [$\delta\rho(\mathbf{r}) = \delta\rho(r)\delta(z)$]:

$$\delta\rho(r) = \int dr' \chi(r, r') \left[V^{\text{ext}}(r') + \int dr'' \frac{e^2 \delta\rho(r'')}{\kappa |r' - r''|} \right], \quad (6)$$

where $\chi(r, r')$ is the susceptibility, which, for circular symmetry, has the form,

we find

$$\delta\rho_m(r) = \int_0^\infty dr' r' [\chi_m(r, r') V_m^{\text{ext}}(r') + \delta\rho_m(r') \beta_m(r, r')], \quad (10)$$

where

$$V_m^{\text{ext}}(r) = \int_0^{2\pi} d\theta V^{\text{ext}}(r) e^{im\theta}, \quad (11)$$

$$\beta_m(r, r') = \frac{4\pi^2 e^2}{\kappa} \int_0^\infty dr'' r'' \chi_m(r, r'') R_m(r', r''), \quad (12)$$

and

direction so that $V^{\text{ext}}(r) = E^{\text{ext}} x = E^{\text{ext}} r \cos\theta$, Eq. (11) becomes

$$V_m^{\text{ext}}(r) = E^{\text{ext}} r \pi (\delta_{m,1} + \delta_{m,-1}). \quad (14)$$

Thus, only modes with $m = \pm 1$ couple to the external radiation. For $B=0$ these modes are degenerate [i.e., $\delta\rho_1(r) = \delta\rho_{-1}(r)$], and Eq. (10) need only be solved for $m=1$. For this case,

$$R_1(r', r'') = \begin{cases} \frac{2}{\pi r'} [K(r'/r'') - E(r'/r'')], & r' < r'' \\ \frac{2}{\pi r''} [K(r''/r') - E(r''/r')], & r' > r'' \end{cases} \quad (15a)$$

$$= \begin{cases} \frac{2}{\pi r'} [K(r'/r'') - E(r'/r'')], & r' < r'' \\ \frac{2}{\pi r''} [K(r''/r') - E(r''/r')], & r' > r'' \end{cases} \quad (15b)$$

We solve Eq. (10) by direct matrix inversion, employing a

modified Simpson's quadrature method to account for the weak singularities of the elliptic integral, K at $r' = r''$.

From the induced charge density we calculate the cross section for photon absorption, $\sigma(\omega)$, given by $\sigma(\omega) = 4\pi(\omega/c)\text{Im}a(\omega)$, where the polarizability $a(\omega)$ is defined as $a(\omega) = (1/E^{\text{ext}})\int d\mathbf{r} x \delta\rho(r)$. In the long-wavelength limit,

$$a(\omega) = \frac{\pi}{E^{\text{ext}}} \int_0^\infty dr r^2 [\delta\rho_1(r) + \delta\rho_{-1}(r)]. \quad (16)$$

As an example we consider the case of a GaAs dot structure for which $m_e = 0.0665m_0$ and $\kappa = 13.1$. We take the disk radius, $R = 1000 \text{ \AA}$, and a jellium density, $n_+ = 4 \times 10^{11} \text{ cm}^{-2}$, which corresponds to ~ 125 positive charges in the disk. For the moment, we neglect the surface states. The number of electrons, n_e , is varied from 1 to 30. The jellium potential $V_+(r)$, is shown in Fig. 1 (dotted line). Near the origin this potential is parabolic, as can be verified by expanding Eq. (2) for small r . For larger r the curvature increases above that of a parabola.

The solid and dashed lines in Fig. 1 illustrate the self-consistent ground-state potential and corresponding electron density for $n_e = 30$. Note that this potential is flat in the region of large electron density where the electrons screen the positive background.¹⁴ The Fermi energy, $\epsilon_f \sim 6.3 \text{ meV}$, 15 spin-degenerate levels are occupied and the energy spacing between the highest occupied and lowest unoccupied levels is around 1.5–2 meV.

The FIR absorption is shown in Fig. 2 for $n_e = 2$ (dotted line), $n_e = 6$ (dashed line), and $n_e = 30$ (solid line). We take the broadening factor, $\gamma = 0.1 \text{ meV}$. For all cases, the spectrum is dominated by a single peak. For small electron number, this peak is very close to the frequency, ω_0 , of the parabolic well defined by the curvature near the origin of the jellium potential, and it is essentially independent of n_e , as has recently been observed in InSb dot structures.² Specifically, expanding Eq. (2) to order r^2 yields, $\omega_0^2 = e^2 \pi n_+ / \kappa m_e R$. In this case, we find $\omega_0 = 4 \text{ meV}$, compared to $\omega \sim 4.2 \text{ meV}$ for the $n_e = 2$ and $n_e = 6$ absorption peaks.

We note that the absorption frequency is significantly larger than the energy-level spacings of the self-consistent ground-state potential, as has been observed in experi-

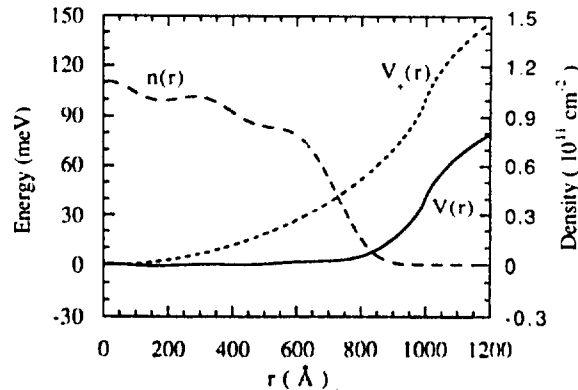


FIG. 1. Bare quantum dot potential, V_+ , (dotted line), as described in the text. Also shown is the self-consistent potential, $V(r)$ (solid line) and electron charge density, $n(r)$ (dashed line) for $n_e = 30$.

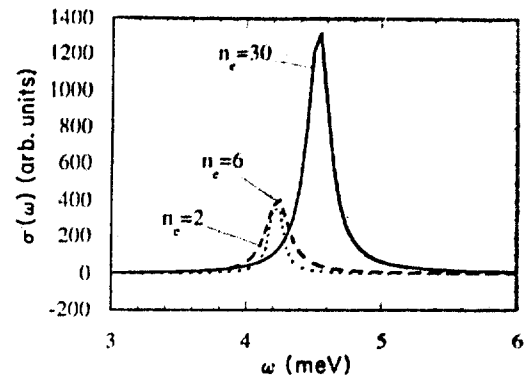


FIG. 2. FIR response of the dot, $\sigma(\omega)$, in the absence of magnetic field for $n_e = 2, 6$, and 30.

ment.³ This large depolarization shift cannot be assigned to any particular single-particle transition since many transitions are involved. In light of the above discussion, it is clearly more appropriate to associate the absorption frequency with the energy spacings of the jellium potential.

For finite magnetic field, the orbital degeneracy is lifted so that the solutions for $m = +1$ and $m = -1$ are different. This leads to a splitting of the single absorption peak into two peaks, which we identify as ω_+ and ω_- , as shown in Fig. 3 for the case of $n_e = 6$. As B increases the ω_- mode decreases in strength while the ω_+ mode increases in strength.² For small electron number, these peaks occur close to the frequencies appropriate for parabolic confinement:

$$\omega_{\pm} = (\omega_0^2 + \frac{1}{4} \omega_c^2)^{1/2} \pm \frac{1}{2} \omega_c, \quad (17)$$

as shown in the inset of Fig. 3.

For large electron number, the absorption shifts to

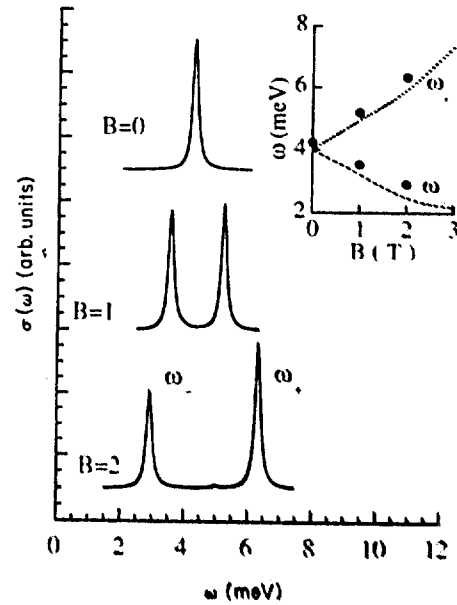


FIG. 3. FIR response, $\sigma(\omega)$, as a function of magnetic field, B . Inset shows the energies of the absorption peaks, ω_+ and ω_- (solid circles) vs B , compared to the strictly parabolic result (dashed lines) of Eq. (18) with $\omega_0 = 4 \text{ meV}$.

higher frequency reaching $\sim 15\%$ deviation from ω_0 for $n_e = 30$ (solid curve of Fig. 2). A similar upward shift in absorption frequencies occurs for finite magnetic field. This shift is related to the changing curvature of the jellium potential with r . As n_e increases so does the spatial extent of the total electron density, which increasingly probes the nonparabolic region of the potential. For small deviations from parabolicity, this idea can be given quantitative formulation by taking the absorption frequency, ω_{eff} , to be defined by the average curvature of the jellium potential:

$$\omega_{\text{eff}}^2 \equiv \frac{1}{2m_e} \langle \nabla^2 V_+ \rangle = - \frac{1}{2m_e} \left\langle \frac{V_+}{R^2 - r^2} \right\rangle, \quad (18)$$

with the average, $\langle \dots \rangle$, taken over the electron charge density, $n(r)$. Applying this formula for $n_e = 30$, we find $\omega_{\text{eff}} = 4.6$ meV, in excellent agreement with the RPA result¹⁵ (solid line in Fig. 2).

We now comment on the effect of occupied surface states. It is evident from a small r expansion of Eq. (3) that the inclusion of surface states increases the curvature of the confining potential and, as a result, enhances the resonance frequency. This in turn enhances slightly the effects of nonparabolicity, for a given n_e . For example, for $n_e = 30$ and $N \sim 95$, we find $\omega_0 = 4.7$ meV and the resonance at $\omega = 5.5$ meV, an upward shift from ω_0 of 17%.

We have also investigated the significance of exchange-correlation effects by including, in the standard fashion, an exchange-correlation model potential, $V_{\text{xc}}(n(r))$, in the local-density approximation (LDA) appropriate for a two-dimensional system.¹⁶ Specifically, for the calculation of the ground state, V_{xc} is added to the V_{eff} entering Eq. (4). Similarly, for the response calculation, a term $(\partial V_{\text{xc}}/\partial n)\delta\rho(r')$ enters the large parentheses of Eq. (6). We find a small downward shift of the response peak whose magnitude decreases with increasing

n_e and is at most 10% of ω_0 . It has been pointed out,¹⁶ however, that two-dimensional calculations for the exchange-correlation energy overestimate substantially the actual exchange-correlation effects in a quasi-two-dimensional system with finite z extent. Therefore, we conclude that these effects do not mask the nonparabolicity effects and modify only slightly the RPA results obtained above. We also have found that for the case of strictly parabolic confinement both the RPA and LDA calculations produce a resonance close (within 1% for $n_e = 30$) to the interlevel separation of the parabola.

As stated above, modes with differing values of m do not couple [see Eq. (10)] because of the circular symmetry of the dot potential. However, once this symmetry is broken, modes with different m can couple, and this coupling should be reflected through the appearance of additional peaks in the FIR absorption spectrum. This mechanism provides a possible explanation for the mode coupling observed in recent FIR measurements on square-shaped dots.³

In summary, we have developed a theory to describe the electromagnetic response of quantum dots, including magnetic field. We find that for small electron number the FIR absorption spectrum corresponds to that associated with parabolic confinement. For large electron number, an upward shift in the resonance frequencies occurs as the electron density probes increasingly the larger curvature of the dot potential. Furthermore, additional effects of nonparabolic confinement such as multiple mode absorption and mode couplings can occur if the dot structures are designed with strongly reduced symmetry and electron occupancy that is sufficiently high to probe the edge asymmetries.

This work was supported in part by the U.S. Army Research Office and the U.S. Office of Naval Research.

¹M. A. Reed, J. N. Randall, R. J. Aggarwal, R. J. Matyi, T. M. Moore, and A. E. Wetsel, Phys. Rev. Lett. **60**, 535 (1988).

²Ch. Sikorski and U. Merkt, Phys. Rev. Lett. **62**, 2164 (1989).

³T. Demel, D. Heitmann, P. Grambow, and K. Ploog, Phys. Rev. Lett. **64**, 788 (1990).

⁴A. Lorke, J. P. Kotthaus, and K. Ploog, Phys. Rev. Lett. **64**, 2559 (1990).

⁵W. Kohn, Phys. Rev. **123**, 1242 (1961).

⁶L. Brey, N. F. Johnson, and B. I. Halperin, Phys. Rev. B **40**, 10647 (1989).

⁷P. A. Maksym and T. Chakraborty, Phys. Rev. Lett. **65**, 108 (1990).

⁸P. Bakshi, D. A. Broido, and K. Kempa, Phys. Rev. B **42**, 7416 (1990).

⁹We mean here either the ionized impurities in the modulation

doped structures or the effective positively charged disk in the periodically gated structures.

¹⁰W. Ekardt, Phys. Rev. Lett. **52**, 1925 (1984).

¹¹A. Kumar, S. E. Laux, and F. Stern, Phys. Rev. B **42**, 5166 (1990).

¹²A. Zangwill and P. Soven, Phys. Rev. A **21**, 1561 (1980).

¹³G. M. Muller, J. Math. Phys. **34**, 179 (1955).

¹⁴This effect has been noted by A. J. Rimberg and R. M. Westervelt, Phys. Rev. B **40**, 3970 (1989), for the case of wide parabolic quantum wells.

¹⁵A similar agreement has been found in the case of a quasi-2D electron gas confined in wide parabolic quantum wells [D. A. Broido, P. Bakshi, and K. Kempa, Solid State Commun. **76**, 613 (1990)].

¹⁶M. Jonson, J. Phys. C **9**, 3055 (1976).